

Superconductivity in the dilute single band limit in reduced Strontium Titanate

Terence M. Bretz-Sullivan^[1], Alexander Edelman^[2], J. S. Jiang^[1], Alexey Suslov^[3],
David Graf^[3], Jianjie Zhang^[4], Gensheng Wang^[4], Clarence Chang^[2,4], John E.
Pearson^[1], Alex B. Martinson^[1], Peter B. Littlewood^[1,2] and Anand Bhattacharya^[1]

[1] *Materials Science Division, Argonne National Laboratory, 9700 S. Cass Avenue, Lemont, IL 60439*

[2] *Department of Physics, The University of Chicago, 5720 South Ellis Avenue, Chicago, IL 60637*

[3] *The National High Magnetic Field Laboratory,*

1800 E. Paul Dirac Drive, Tallahassee, FL 32310

[4] *High Energy Physics Division, Argonne National Laboratory, 9700 S. Cass Avenue, Lemont, IL 60439*

(Dated: March 26, 2025)

Strontium titanate is a multi-band low carrier density superconductor. In the single occupied band limit, we find that a zero resistance state can be obtained in reduced $\text{SrTiO}_{3-\delta}$ single crystals at carrier densities as low as $n = 1.03 \times 10^{17} \text{cm}^{-3}$, and a partial resistive transition is observed for $n = 3.85 \times 10^{16} \text{cm}^{-3}$. We observe low critical current densities, relatively high and isotropic upper critical fields, and an absence of diamagnetic screening. The resistive transition is inconsistent with a homogeneous superconducting state, accounting for fluctuations. Our observations suggest an inhomogeneous superconducting state embedded within a 3-dimensional electron gas.

Since the 1960s, superconductivity in electron-doped SrTiO_3 (STO) has attracted much attention.[1, 2] It was the earliest example of a ‘dome’ in the superconducting phase diagram, with relatively low carrier densities (n) in the range $6.9 \times 10^{18} \text{cm}^{-3} < n < 5.5 \times 10^{20} \text{cm}^{-3}$. [3] More recently, it was shown that superconductivity occurs in reduced STO single crystals with $n < 1.5 \times 10^{18} \text{cm}^{-3}$, where only a single band is occupied in a 3-dimensional (3D) electron gas.[14, 15] Upon populating the lowest band, a maximum $T_c \sim 200$ mK was observed just as the Fermi level E_F reaches the bottom of the second band, thus revealing a second dome in T_c vs n , where superconductivity was found to persist down to $n = 5.5 \times 10^{17} \text{cm}^{-3}$. These carrier densities are comparable to that for crystalline Bi, a superconductor with $T_c \sim 0.5$ mK, with the lowest known carrier density of $n \approx 3 \times 10^{17} \text{cm}^{-3}$. [7]

In this work, we report on superconductivity in $\text{SrTiO}_{3-\delta}$ in the single band limit in the density range $3.85 \times 10^{16} \text{cm}^{-3} < n < 1.37 \times 10^{18} \text{cm}^{-3}$, including densities much lower than previously reported.[14, 15] Our magnetotransport measurements reveal single frequency Shubnikov-de Haas (SdH) oscillations. These SdH frequencies are consistent with a single spherical Fermi surface with carrier densities that agree with those inferred from Hall measurements, implying a homogeneous 3D electron gas in the single band limit. Furthermore, in this regime we find that superconducting $\text{SrTiO}_{3-\delta}$ has very low critical current densities, several orders of magnitude smaller than the depairing current. This is accompanied by an absence of diamagnetic screening, and isotropic and substantially high upper critical fields ($\mu_0 H_{c2}$). Our data suggest that in the single band limit in $\text{SrTiO}_{3-\delta}$ the normal state carriers form a homogeneous 3D electron gas, while the superconducting state is inhomogeneous.

Superconductivity in STO is derived from electrons pairing in three bands in the Ti 3d t_{2g} manifold.[4] At

low temperatures, the three degenerate bands are split at the Γ -point by a combination of spin-orbit interaction, and octahedral rotations that lead to a tetragonal distortion. Upon increasing the Fermi level through doping via chemical substitution or by introducing oxygen vacancies, electrons sequentially populate these three bands. STO is also an incipient ferroelectric at low temperatures with a static dielectric constant $> 20,000$. [5] As a result, when doped it remains metallic down to very low carrier densities with relatively high mobilities in high quality bulk single crystals and thin films.[6, 8–11]

The essential difficulties in understanding superconductivity in this low- n limit are captured in the BCS expression for the transition temperature $T_c \sim \Theta_D \exp(-1/N(0)V)$. [37] Here the Debye temperature Θ_D comes from a cutoff energy in the gap equation, set by knowledge of the characteristic scales of the microscopic mechanisms of electron attraction and repulsion, which remain hotly debated in STO.[3, 19, 22, 23, 27] The attractive pairing interaction strength V must compensate for the low density of states $N(0)$ at these doping levels, so that the system does not necessarily flow to the usual BCS weak-coupling fixed point, opening the possibility of a crossover to a BEC state with exotica such as preformed pairs.[13, 45] Similarly, the energy scales Ω of many possible pairing interactions are anti-adiabatic, $\Omega \gg E_F$, where pairing involving a retarded attractive interaction does not apply, there is no Migdal’s theorem, and perturbative calculations are questionable. Thus it is remarkable that tunneling and microwave measurements reveal a perfectly ordinary single-gap superconductor with a weak BCS coupling constant, smaller than that of aluminum, and a BCS like Δ/T_c , though we note that these measurements were carried out on samples with $n > 1.0 \times 10^{19} \text{cm}^{-3}$. [28, 35, 36]

All six samples in this study show signatures of superconductivity with a high mobility and metallic behav-

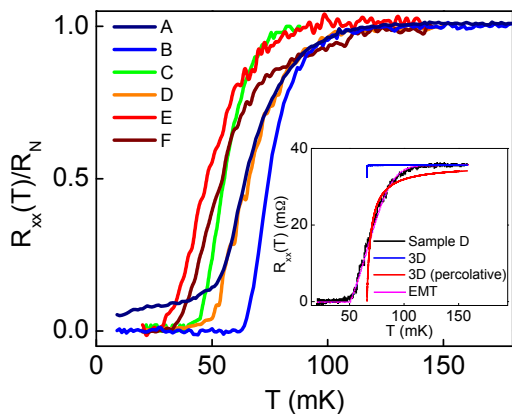


FIG. 1: $R_{xx}(T)$ for the samples listed in Table 1. Inset: Paraconductivity (σ') fits to Sample D, as explained in the text.

ior in the normal state. For sample preparation, measurement details and high temperature measurements see Supplemental Material. In Fig. 1, we plot $R_{xx}(T)$, normalized to the normal state resistance R_N , for all samples in zero magnetic field. Five of the samples exhibit a complete superconducting transition with the highest onset temperature of 115 mK in Sample F. We note that T_c does not follow n . Sample B has both the largest T_c of our set and nearly a fifth of the previous lowest carrier density at which superconductivity has been observed in reduced STO.[14, 15] On the other hand, the T_c 's of our samples are not as high as previously reported at similar doping levels.[14, 15]

At $n = 3.85 \times 10^{16} \text{ cm}^{-3}$, Sample A exhibits an incomplete transition. $R_{xx}(T)$ falls sharply below T_c to $< 0.2 \times R_N$, similar to Sample D, but then has a resistive tail below 50 mK going down to $\sim 0.05 \times R_N$ at 10 mK. This resistive transition and tail is reminiscent of behavior seen in ultrathin films of quenched deposited metals just on the threshold for global superconductivity,[32, 33] which were modeled as a network of Josephson coupled superconducting grains. Global phase coherence occurs when the resistive dissipation between grains falls below \hbar/e^2 and is macroscopically tuned via R_N , which parameterizes static disorder.[32, 33] It is possible that Sample A with the lowest n and highest R_N values amongst all our samples is just beyond the percolative limit for superconductivity in STO.

All of our samples exhibit Shubnikov-de Haas (SdH) oscillations in $R_{xx}(\mu_0 H)$ periodic in $1/\mu_0 H$, as each Landau level is swept through the Fermi energy. (Fig. 2 inset, and Supplemental Material). We extract the oscillations (δR_{xx}) by fitting the minima of the magnetoresistance traces with a fourth order polynomial in $\mu_0 H$, and subtracting this polynomial fit from the raw data. The SdH oscillation period is related to the cross sectional area of the Fermi surface and thus the density of electrons

Sample	n (10^{17} cm^{-3})	μ ($\text{cm}^2/\text{V-s}$)	ρ_N ($\text{m}\Omega\text{-cm}$)	T_c (mK)
A	0.385	13,712	18.63	65
B	1.03	8,676	8.10	75
C	2.40	28,978	0.63	55
D	6.59	27,100	0.45	66
E	9.89	23,520	0.26	48
F	13.68	32,384	0.24	55

TABLE I: Sample Parameters. n and μ are the Hall carrier density and mobility respectively. ρ_N is the normal state resistivity. T_c is defined at half the normal state resistance.

in 3D by $\Delta(1/\mu_0 H) = (\frac{16}{9\pi})^{1/3} \frac{n_{SdH}^{-2/3}}{\Phi_0}$. Here $\Phi_0 = \pi \hbar/e$ is the flux quantum, and we assume a spherical Fermi surface. The single frequency observed in SdH oscillations is consistent with a single, small electron pocket contributing to transport, where the oscillation at the highest fields show evidence of spin splitting.[16] Additionally, in Fig. 2, we compare the measured Hall densities n to n_{SdH} to determine the homogeneity of the 3D electron gas underlying the superconducting state. n is inferred by assuming a homogeneous electron gas through the thickness of the sample. At larger carrier densities, n_{SdH} deviates from n as the onset of filling a second band begins.[14, 15] We note that in earlier measurements on a sample with a lower carrier density $n = 1.05 \times 10^{17} \text{ cm}^{-3}$, we showed that the SdH oscillations for magnetic fields applied in-plane and out-of-plane of the sample had nearly identical frequencies.[9] This is consistent with a 3D Fermi surface symmetric about the principal axes.

Next, we examine the upper critical field ($\mu_0 H_{c2}$) of our samples in the low field magnetoresistance, where we

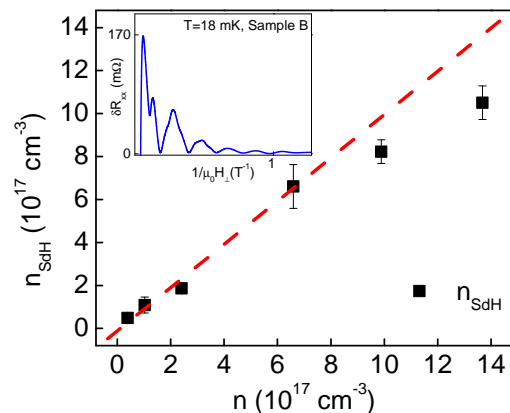


FIG. 2: A plot of n_{SdH} vs n for each sample in Table 1. The red dashed line is a guide for $n_{SdH} = n$. Inset: Shubnikov-de Haas oscillations in Sample B.

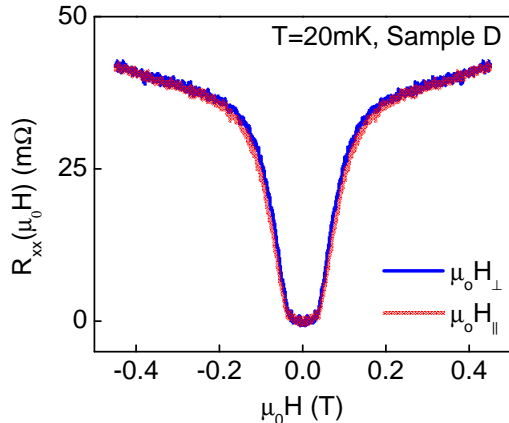


FIG. 3: Low field $R_{xx}(T = 20\text{mK}, \mu_0H)$ for Sample D which exhibits an isotropic upper critical field.

define μ_0H_{c2} at $R_N/2$. As shown for Sample D (Fig. 3), the $R_{xx}(\mu_0H)$ sweeps are nearly the same for magnetic field orientations either out-of-the-plane (blue trace - μ_0H_{\perp}) or in-plane and parallel with the applied current (red trace - μ_0H_{\parallel}) (for other samples, see Supplemental Material). We completely suppress superconductivity at $\mu_0H = 0.2\text{T}$. For $\mu_0H \lesssim 0.2\text{T}$, the finite slope at higher magnetic field values is due to the positive magnetoresistance of our samples in their normal state. If superconductivity in the very low n limit were an artifact due to a 2D layer of oxygen vacancies in a near-surface region of the order of the London penetration depth λ or thinner, μ_0H_{c2} would be enhanced in-plane relative to the out-of-plane value due to the absence of diamagnetic screening.[31] Since this is not the case, our data are consistent with superconductivity permeating the bulk of the sample, and not confined to $\sim \lambda$ from the surface. A simple estimate of λ , using London theory, would suggest $7\ \mu\text{m} < \lambda < 33\ \mu\text{m}$ (Supplemental Material). However, as we will comment on later, measuring λ of these samples, is not possible since they do not show signatures of screening of magnetic fields.

The measured values of μ_0H_{c2} (Fig. 4b) in our samples (barring the lowest doped sample) are significantly larger than measured in optimally doped Nb-STO, with much higher carrier densities of $n = 2.6 \times 10^{20}\text{cm}^{-3}$, where $\mu_0H_{c2} = 0.048\text{T}$. [24] Prior measurements on underdoped reduced STO samples, with carrier densities in the $n = 10^{18} - 10^{19}\text{cm}^{-3}$ range ($100\text{mK} < T_c < 230\text{mK}$) [25] also find larger values of μ_0H_{c2} , in the range of 0.3 - 0.4 T. Our reduced STO samples have lower doping, lower T_c and lower μ_0H_{c2} values than these samples.

A key finding of our work is the anomalously low critical current density (J_c) as seen in Fig. 4(a,b). We determine I_c from the maxima in dV/dI vs. I_{DC} , denoted by the vertical black dashed line, and compute J_c assuming

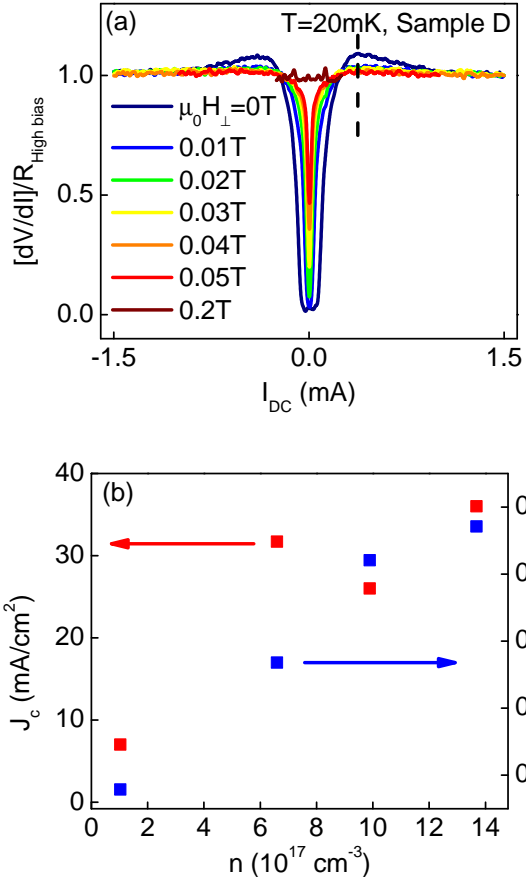


FIG. 4: J_c and μ_0H_{c2} measurements and results in the single band limit. (a) dV/dI vs. I_{DC} measurements in Sample D with the suppression of I_c as a function of magnetic field. The vertical dashed line corresponds to I_c . Each trace is normalized to 1 by the value of dV/dI at $I_{DC,max}$, $R_{High\ bias}$. (b) Low J_c and large μ_0H_{c2} vs n : J_c falls considerably at lowest carrier densities.

that the supercurrent is uniformly distributed across the device. We find $7 \times 10^{-3}\text{A/cm}^2 < J_c < 36 \times 10^{-3}\text{A/cm}^2$. The magnitude of J_c is less than the estimated depairing current density by 10^4 (Supplemental Material). The rapid suppression of J_c at lowest doping, with relatively small variations in T_c , is suggestive of the onset of a percolative threshold with reduced carrier density, below which regions of similar T_c fail to form a connected cluster that spans the measurement leads. Analogous to the magnetoresistance measurements in Fig. 3, we suppress I_c completely and isotropically at $\mu_0H = 0.2\text{T}$. We note that $J_c \sim 10^2\text{A/cm}^2$ have been reported in reduced STO single crystals in earlier work.[25] However, these values of J_c are higher than that in our highest doped samples by $\sim 3 \times 10^4$ while the carrier density estimated from T_c values in these samples is only ~ 10 times higher. These results suggest that our samples are close to a percolative

threshold for superconductivity.

Another anomaly in our data is the width of the superconducting transition, ΔT_c . In 3D, the excess conductivity due to superconducting fluctuations in a homogeneous superconductor above T_c , $\sigma' \propto \epsilon^{-1/2}/\xi$, is a universal function of the reduced temperature $\epsilon = (T - T_c)/T_c$ scaled by the superconducting coherence length ξ [38, 39], which we obtain from our measurements of H_{c2} . As shown in the inset of Fig. 1, this expression grossly underestimates the width of the transition. To incorporate the effects of a possible percolative state, we follow Char and Kapitulnik[42] in considering a static percolating network of fixed T_c embedded in a bulk sample that remains normal. Here, superconducting fluctuations probe the underlying physical dimension of the system down to a percolative length scale ξ_p , below which the fractal dimension of percolation $d_p = 4/3$ controls the paraconductivity, producing $\sigma'_{AL} \propto \epsilon^{-4/3}$. Non-universal corrections [40, 41] are also more prominent at these short wavelengths. Although the parameter values that best fit the transition are physically reasonable, i.e. $\xi_p \sim 10\xi$, we do not obtain qualitative agreement with the data. (see Supplemental Materials for details of fits, also considering other possible fluctuation dimensions). In general, the measured paraconductivity decays more quickly at high temperatures than any power-law fluctuation theory (or crossover between power laws), whereas naively one would have enhanced thermal fluctuations from the fact that $\Delta T_c \sim T_c$. Schematically, we may attribute this to the fact that the percolative network is not fixed, but in fact grows and crosses the percolation threshold as the temperature is lowered. Lastly, we use a model in which the T_c of sites is drawn from a Gaussian distribution of width σ . Using an effective medium approximation[47, 48] and a suitably chosen ΔT_c and T_c , we are able to reproduce the shape of the resistive transition, although some samples display slight excess conductivity at intermediate temperatures (see Supplemental Material). T_c and σ vary unsystematically with the doping, although their precise values depend on the assumed percolation geometry (we use 3D simple cubic site percolation). The fact that each doping realization seems to produce a different macroscopic T_c is difficult to explain away as a finite-size effect, due to the absence of resistive jumps (exceeding our noise limit) in the data. Finally, we note that the residual unexplained conductance in some of the samples leaves open some role for fluctuations in a reduced dimension, for instance if superconductivity localizes preferentially on domain walls, which would be consistent with the observed low critical currents.

At the lower doping levels in STO ($n < 6.9 \times 10^{18} \text{cm}^{-3}$), there has been no evidence for Meissner screening,[2, 19, 24] a pre-requisite for establishing a homogeneous superconducting state. We attempted to measure changes in λ of an unpatterned piece of Sam-

ple E using a tunnel diode oscillator (TDO) setup down to 20 mK. We were unable to resolve any signatures of a bulk superconducting transition (Supplemental Material), while we were able to do so in a LuPdBi sample, another low carrier density superconductor, using the same setup.[46] Thus, to the best of our knowledge our samples do not show any diamagnetic screening in the superconducting state. This result is consistent with early measurements on reduced STO [3] where diamagnetic screening could not be observed for $n < 6.9 \times 10^{18} \text{cm}^{-3}$, and in Nb-STO for $n < 4.1 \times 10^{19} \text{cm}^{-3}$. [24]

Taken together, the data presented here suggest a superconducting state where the superfluid density is inhomogeneously distributed in regions of $\xi < l_{sc} < \lambda$ that permeate the sample. The agreement between carrier densities obtained from Hall and SdH oscillation measurements suggest the normal state is nearly homogeneous in the bulk of the sample. The lack of diamagnetic screening suggests that the superconductivity is confined to regions smaller than λ in at least one dimension. Nonetheless, the relatively high values of $\mu_0 H_{c2}$ indicate that the superconducting state has a well developed gap. Our data are consistent with a percolative transition as different such regions go superconducting, with onset of superconductivity near T_c being representative of an ensemble property, and I_c in the zero-resistance state being set by the weakest links. This would depend on the particular disorder realization in the sample, which is consistent with our finding of unsystematic variations of T_c with density.

A possible origin of such an inhomogeneous superconducting state within a homogeneous 3-D electron gas could be linked to the tetragonal domain walls that permeate and intersect throughout the bulk of our samples. These domain walls could be electronically distinct from the bulk and may favor superconductivity. This may be similar to LAO/STO devices where superconductivity was found to be modulated by domain walls in STO [43], or localized near the edges of the gated areas in quasi 1-D channels, which was also attributed to domain walls at the channel edges.[30] Real space imaging of partial diamagnetic screening from our samples may provide valuable clues about the spatial nature of this unusual superconducting state.[43, 44]

In conclusion we observe superconductivity in single crystals of reduced SrTiO₃ at lower carrier densities than previously reported.[14, 15] The isotropic critical field, low critical current density and lack of diamagnetic screening are suggestive of an inhomogeneous superconducting state in the bulk of the sample, where the threshold for a resistive transition to superconductivity is near the unusually low carrier density of $n \sim 5 \times 10^{16} \text{cm}^{-3}$.

All work at Argonne (sample preparation, transport and structural characterization, theoretical analysis) were supported by the the U.S. Department of Energy, Office of Science, Basic Energy Sciences, Materials

Science and Engineering Division. We acknowledge the contributions from Gensheng Wang, Clarence Chang and Jianjie Zhang in assisting with low temperature transport measurements. Use of the Center for Nanoscale Materials, an Office of Science user facility, was supported by the U.S. Department of Energy, Office of Science, Office of Basic Energy Sciences, under Contract No. DE-AC02-06CH11357. Dilution fridge based transport and TDO measurements in magnetic fields were performed at the National High Magnetic Field Laboratory, which is supported by National Science Foundation Cooperative Agreement No. DMR-1157490 and DMR-1644779 and the State of Florida. We also thank Carley Paulsen at the Institut Néel for his dilution fridge based SQUID magnetometry measurements.

-
- [1] J. F. Schooley, W. R. Hosler, and M.L. Cohen, *Phys. Rev. Lett.* **12**, 474 (1964).
- [2] J. F. Schooley, W. R. Hosler, E. Ambler, J. H. Becker, M.L. Cohen and C. S. Koonce, *Phys. Rev. Lett.* **14**, 305 (1965).
- [3] C. S. Koonce, M. L. Cohen, J. F. Schooley, W. R. Hosler, and E. R. Pfeiffer, *Phys. Rev.* **163**, 380 (1967).
- [4] L. F. Mattheiss, *Phys. Rev. B* **6**, 4740 (1972).
- [5] K. A. Müller and H. Burkard, *Phys. Rev. B* **19**, 3593 (1979).
- [6] X. Lin, B. Fauqué, K. Behnia, *Science* **349**, 945 (2015).
- [7] O. Prakash, A. kumar, A. Thamizhavel and S. Ramakrishnan, *Science* **355**, 52 (2017).
- [8] A. Spinelli, M.A. Torija, C. Liu, C. Jan and C. Leighton, *Phys. Rev. B* **81**, 155110 (2010).
- [9] A. Bhattacharya, B. Skinner, G. Khalsa, A. Suslov, *Nature Communications* **7**, 12974 (2016).
- [10] J. Son, P. Moetakef, B. Jalan, O. Bierwagen, N. J. Wright, R. Engel-Herbert and S. Stemmer, *Nature Materials* **9**, 482 (2010).
- [11] Y. Kozuka, M. Kim, H. Ohta, Y. Hikita, C. Bell and H.Y. Hwang, *Appl. Phys. Lett.* **97**, 222115 (2010).
- [12] R.J. Tainsh and C. Andrikidis, *Solid State Commun.* **60**, 517 (1986).
- [13] D.M. Eagles, *Solid State Commun.* **60**, 521 (1986), D.M. Eagles, R.J. Tainsh, and C. Andrikidis, *Physica C* **157**, 48 (1989).
- [14] X. Lin, G. Bridoux, A. Gourgout, G. Seyfarth, S. Krämer, M. Nardone, B. Fauqué, and K. Behnia, *Phys. Rev. Lett.* **112**, 207002 (2014).
- [15] X. Lin, Z. Zhu, B. Fauqu, and K. Behnia, *Phys. Rev. X* **3**, 021002 (2013).
- [16] S. J. Allen, B. Jalan, S.-B Lee, D. G. Ouellette, G. Khalsa, J. Jaroszynski, S. Stemmer and A. H. MacDonald *Phys. Rev. B* **88**, 045114 (2013).
- [17] N. Reyren, S.Thiel, A. D. Caviglia, L. Fitting Kourkoutis, G. Hammerl, C. Richter, C.W. Schneider, T. Kopp, A.-S. Rüetschi, D. Jaccard, M. Gabay, D.A. Muller, J.-M. Triscone and J. Mannhart, *Science* **317**, 1196 (2007).
- [18] J.-F. Ge, Z.-L. Liu, C. Liu, C.-L. Gao, D. Qian, Q.-K. Xue, Y. Liu and J.-F. Jia, *Nature Materials* **14**, 285 (2015).
- [19] M. L. Cohen, *Phys. Rev.* **134**, A511 (1964).
- [20] L. V. Gurevich, A. I. Larkin, and Y. A. Firsov, *Sov. Phys. Sol. State* **4**, 131 (1962).
- [21] Y. Takada, *J. Phys. Soc. Jpn.* **45**, 786 (1978).
- [22] J. Ruhman and P.A. Lee, *Phys. Rev. B* **94**, 224515 (2016).
- [23] P. Wolffe and A. V. Balatsky, *Phys. Rev. B* **98**, 104505 (2018).
- [24] C. Collignon, B.Fauqué, A. Cavanna, U. Gennser, D. Mailly, and K. Behnia *Phys. Rev. B* **96**, 224506 (2017).
- [25] M. Jourdan, N. Blumer and H. Adrian, *Eur. Phys. J. B* **33**, 25 (2003).
- [26] J. M. Edge, Y. Kedem, U. Aschauer, N.A. Spaldin and A. V Balatsky, *Phys. Rev. Lett.* **115**, 247002 (2015).
- [27] L.P.Gorkov, *Proc. Nat. Acad. Sci.* **113**, 4646 (2016).
- [28] G. Binnig, A. Baratoff, H. E. Hoening, and J. G. Bednorz, *Phys. Rev. Lett.* **45**, 1352 (1980).
- [29] D. van der Marel, J. L. M. van Mechelen, and I. I. Mazin, *Phys. Rev. B* **84**, 205111 (2011).
- [30] Y.-Y. Pai, H. Lee, J.-W. Lee, A. Annadi, G. Cheng, S. Lu, M. Tomczyk, M. Huang, C.-B. Eom, P. Irvin and J. Levy, *Phys. Rev. Lett.* **120**, 147001 (2018).
- [31] M. Tinkham, *Introduction to Superconductivity*, Second Edition, Dover Publications, Inc., Mineola, NY (2004).
- [32] H. M. Jaeger, D. B. Haviland, A. M. Goldman and B. G. Orr, *Phys. Rev. B* **34**, 4920(R) (1986); H. M. Jaeger, D. B. Haviland, B. G. Orr and A. M. Goldman, *Phys. Rev. B* **40**, 182 (1989).
- [33] B. G. Orr, H. M. Jaeger and A. M. Goldman, *Phys. Rev. B* **32**, 7586(R) (1985).
- [34] O. Entin-Wohlman, A. Kapitulnik, S. Alexander and G. Deutscher, *Phys. Rev. B* **30**, 2617 (1984).
- [35] A. G. Swartz, H. Inoue, T. A. Merz, Y. Hikita, S. Raghu, T. P. Devereaux, S. Johnston, and H. Y. Hwang, *PNAS* **115**, 1475 (2018).
- [36] M. Thiemann, M. H. Beutel, M. Dressel, N. R. Lee-Hone, D. M. Broun, E. Fillis-Tsirakis, H. Boschker, J. Mannhart and M. Scheffler, *Phys. Rev. Lett.* **120**, 237002 (2018).
- [37] J. Bardeen, L. N. Cooper, and J. R. Schrieffer, *Phys. Rev.* **108**, 1175 (1957).
- [38] W. J. Skocpol and M. Tinkham, *Rep. Prog. Phys.* **38**, 1049 (1975).
- [39] L. G. Aslamasov and A. I. Larkin, *Phys. Lett. A* **26**, 238 (1968).
- [40] K. Maki, *Prog. Theor. Phys.* **40**, 193 (1968).
- [41] R. S. Thompson, *Physica* **55**, 296 (1971).
- [42] K. Char and A. Z. Kapitulnik, *Physik B - Cond. Matt.* **72**, 253 (1988).
- [43] H. Noad, P. Wittlich, J. Mannhart and K. A. Moler arXiv:1805.08549v1.
- [44] J. A. Bert, B. Kalisky, C. Bell, M. Kim, Y. Hikita, H. Y. Hwang and K. A. Moler, *Nature Physics* **7**, 2079 (2011).
- [45] G. Cheng, M. Tomczyk, S. Lu, J. P. Veazey, M. Huang, P. Irvin, S. Ryu, H. Lee, C.-B. Eom, C. S. Hellberg, and J. Levy, *Nature* **521**, 196 (2015).
- [46] Y.Nakajima, R. Hu, K. Kirshenbaum, A. Hughes, P. Syers, X. Wang, K. Wang, R.Wang, S. R. Saha, D. Pratt, J.W. Lynn, J. Paglione, *Sci. Adv.*, **1**, 5 (2015).
- [47] [P. Popevi, D. Pelc, Y. Tang, K. Velebit, Z. Anderson, V. Nagarajan, G. Yu, M. Poek, N. Bariii, and M. Greven, *Npj Quant Mater* **3**, 42 (2018).
- [48] M. Nakamura, *Phys. Rev. B* **29**, 3691 (1984).